DOI: https://doi.org/10.57233/ijsgs.v11i3.932

ISSNp: 2488-9229; ISSNe: 3027-1118

IJSGS FUGUSAU VOL. 11(3) WEBSITE: https://fugus-ijsgs.com.ng

INTERNATIONAL JOURNAL OF SCIENCE FOR GLOBAL SUSTAINABILITY
(A PUBLICATION OF FACULTY OF SCIENCE, FEDERAL UNIVERSITY GUSAU, NIGERIA)

Suction/Injection Effect on Exponential Heat Generating Fluid Via a Slit Microchannel

Abubakar Muhammad Tsafe[1]*, Muhammed Murtala Hamza[2], Halima Usman[3], Godwin Ojemeri[4], Abdullahi Manniru Galadima[5] and Umar Ishaq Rano[6]

[1,2,3,5]Department of Mathematics, Faculty of Physical and Computing Sciences, Usmanu Danfodiyo University, P. M. B. 2346 Sokoto State, Nigeria.

[4]Department of Mathematics, College of Science, Federal University of Agriculture, Zuru, P. M. B. 28, Kebbi State, Nigeria.

[6]Department of Business Administration, Faculty of Social Sciences, Usmanu Danfodiyo University, P. M. B. 2346 Sokoto State, Nigeria.

***Corresponding Author's Email**: amtsafe101@gmail.com

Received on: August, 2025 **Revised and Accepted on:** September, 2025 **Published on:** October, 2025

ABSTRACT

In this article, the impacts of magnetic fields and fluid motion with exponential heat generation inside a slit porous microchannel affected by suction/injection impact are investigated analytically. We analyzed the natural convective flow of an incompressible fluid over a parallel plate microchannel exposed to a perpendicular magnetic field. One of the parallel plates has a superhydrophobic surface (SHS), while the other plate has a no-slip surface (NSS). A closed-form approach was employed to treat the governing equations for case I, representing the physical scenario of a heated SHS while the NSS remained unheated, and case II, depicting the realistic conditions where a no-slip wall is heated while the SHS remains unheated. The consequences of various flow parameters, such as suction/injection, Darcy number (Da), exponential heat generating parameter (Qg), and MHD, on velocity and temperature, volume flow rate, skin friction, and Nusselt number are graphically demonstrated. It is concluded that the action of suction/injection is to decrease/increase the temperature and velocity components, respectively, for both cases. It is revealed that thermal profiles rise in both cases, considering the impact of the exponential heat generation parameter (Qg). The velocity component and volume flow rate substantially increased with the influence of the Darcy number (Da) and the exponential heat source parameter (Qg). This work will encourage the advancement of knowledge in fluid dynamics and heat transfer, with possible uses for heat transfer advances in the chemical and engineering sectors, microelectronic cooling/heating, biomedical devices, and lab-on-a-chip devices.

Keywords: Exponential heat source, Suction/injection, Magnetohydrodynamics (MHD), Porous material, Slit Microchannel.

1.0 INTRODUCTION

A planar layer or channel surface with porosity or passageways that let fluid leak will experience suction or injection. In the management of the boundary layer region, particularly in engineering, aerodynamics, space technology, and medical sciences, the suction/injection impact is very crucial. These applications prompted our quest to dig further into the effect of suction/injection in industrial working fluids. References such as Mishra *et al.* (2022), Chaudhary and Jain (2007), and Khalid *et al.* (2015) explain the demonstrations of this concept. Given this, Hamza *et al.* (2024c) explored the effect of wall porosity on unsteady magnetized slip flow affected by temperature-dependent thermal property and asymmetric/symmetric wall heating in an upward-facing channel. Jha *et al.* (2022) studied the outcomes of injection or suction on buoyancy-induced flow in an upward channel due to a point/line heat sink/source using the Laplace transform technique. Uwanta *et al.* (2014) analysed the action of wall suction/injection on magnetized buoyancy-induced flow in an up-facing plate. It was established that fluid velocity can be effectively regulated by injection or suction. The significance of suction/injection on magnetized natural convection was expounded by Jha *et al.* (2018). Additionally, Jha *et al.* (2019) investigated how buoyancy-induced flow is affected by suction and injection. They found that the fluid motion is lowered by raising the injection parameter. Also, the suction parameter goes up, and so do the shear stress characteristics. Kamis *et al.* (2021) investigated heat flow analysis in the blood fluid-based copper and alumina nano elements across a transient stretching sheet affected by suction/injection. Other works that provided some comprehensive insights into the impacts of unsteady magnetized hybrid nanofluid flow across a stretching or shrinking thin film with suction/injection effects can be seen in references Kamis *et al.* (2023), Kamis *et al.* (2022), Bachock *et al.* (2023), and Karouei *et al.* (2024).

Magnetized flows with heat transfer features in porous media have been largely explored in recent times owing to their significance in numerous engineering processes, namely liquid metal separation, metallurgy, compact heat exchangers, and fusion control. A good number of authors have accomplished quality works to exemplify this phenomenon. In this regard, Adeyemo *et al.* (2024) modelled a numerical study on the thermally and chemically transfer characteristics of a

DOI: https://doi.org/10.57233/ijsgs.v11i3.932 ISSNp: 2488-9229; ISSNe: 3027-1118
IJSGS FUGUSAU VOL. 11(3) WEBSITE: https://fugus-ijsgs.com.ng

nonlinear convective heat source fluid flow affected by variable viscosity and porosity impacts. The research examined the interplay between variable viscosity, porous medium properties, and heat emission on fluid flow, heat transfer, and mass transport, shedding light on the complex relationships between these factors. The findings offer valuable insights into optimizing energy and mass flux processes in various porous media applications. Ajibade *et al.* (2023) discussed the implications of viscous and Darcy dissipation on MHD free flow over a slit channel partially filled with porous material affected by heat generation, using the homotopy perturbation method. Ojemeri and Onwubuya (2023c) emphasized the consequences of viscous dissipation and porosity factors on magnetized buoyancy-induced flow of an incompressible fluid traveling along a slit microchannel that is alternately heated and equipped with SHS and temperature jump conditions. Nihall *et al*. (2024) examined the thermally and chemically propelled flow in a nanofluid over a radially elastic sheet, taking into account the effects of activation energy. Their results show that increasing the exponential heat source or sink leads to difficulty in effectively transporting heat, thereby reducing the heat transfer amount. Fathi *et al*. (2023) investigated the thermal performance of porous-fin microchannel heat sinks for the cooling of advanced micro-electronics. Their numerical study examined how porosity, fin thickness, and fluid flow affect heat transfer rates. The results indicated that porous-fin microchannels markedly encourage heat transfer rates and decrease thermal resistance, presenting a promising solution for cooling high-power micro-electronics. Chakravarty *et al*. (2022) examined the consequences of liquid coolant sub-cooling on boiling heat transfer with porous media through numerical simulations utilising a two-phase flow model. Their findings revealed that subcooling significantly improves boiling heat transfer rates and postpones drying out. The study identified optimal levels of subcooling that maximize heat transfer while minimizing the risk of drying out. Allan and Dardery (2018) outlined the impact of chemically and thermally driven flow on a time-dependent mixed convection flow across an upstanding porous channel. Bordoloi *et al*. (2021) gave the interpretation of the diffusion-thermo effect on a three-dimensional flow through a porous upstanding plate in a porous medium affected by a periodic suction factor. Other references that provided more insight into the concept under consideration can be found in Hamza *et al*. (2022), Bordoloi *et al.* (2023), Kadeethum *et al*. (2022), and Gireesha and Sindu (2020), to cite a few.

In heat transfer analysis, the study of fluid flow in microchannels with SHO characteristics and jump temperature is a fundamental one of long interest. Some of the features of microchannels with SHS are extremely water repellent, self-cleaning mechanisms, reduced friction, and enhanced flow. Lee *et al*. (2021) opined that microchannels with SHS can minimize the effect of water exposure on surfaces and enable self-cleaning behaviour. Microchannels with SHS have found applications in the creation of lab-on-a-chip medical diagnostic devices, regulated microfluidic transport, heat transfer augmentation through effective liquid flow, and oil and water separation in microfluidic structures. Akhtari and Karimi (2020) mentioned that SHS used in microchannels can minimize the pumping power needed to initiate the fluid's speed. A good number of outstanding authors have greatly contributed to the studies of different effects in microchannels influenced by SHS. To this end, Ojemeri *et al*. (2024) underscored the significance of the heat source/sink on chemically reactive fluid flow in a SHO-heated microchannel using a semi-analytical method. Hamza *et al*. (2024a, 2024b) reported the influence of electrokinetic effects on free and combined flows in SHO microchannels and a temperature jump scenario. It is revealed from their analytical result that the function of the SHS and electrokinetic features is to enhance the fluid motion in the microchannel. Hamza *et al.* (2025) studied the impact of heat generating fluid in a superhydrophobic microchannel affected by velocity slip and temperature jump conditions. In the field of MHD, Jha and Gwandu (2018, 2020) studied fluid flow in the application of a magnetic intensity in an up-facing microchannel coated with SHO conditions, porous medium, and temperature jump. Yale *et al*. (2023) explored the function of viscous dissipative fluid in a slit microchannel with SHS. Ojemeri and Onwubuya (2023a, 2023b) examined this phenomenon with mixed convection flow affected by porous medium and chemically propelled heat source or sink fluid in a SHO microchannel. Sharma *et al*. (2020) provided a theoretical simulation that describes the pressure-driven flow along a microchannel involving SHS characteristics with constant heat flux. Other interesting research with different thermal boundary scenarios with SHS can be seen in these references: Sia *et al.* (2023), Heidarian *et al*. (2020), and Zhang *et al*. (2019).

The study of fluid suction or injection flow is of crucial importance for medical sciences as well as technical applications such as the cooling and drying of paper and textiles and the extrusion of metals and polymers, to name a few. It is used in particular for problems with blood circulation, blood flow, cancer treatment, aerodynamics, and so on. These developments have been made possible by the use of improved working fluids, novel channel walls with enhanced heat insulation features, or inventive geometric designs. Therefore, this paper intends to build on the contribution of Hamza *et al.* (2025) by incorporating the novel and interesting interactions between suction/injection, exponential heat generation, and porous SHO microchannel features on fluid flow patterns and thermal characteristics. The results from

DOI: https://doi.org/10.57233/ijsgs.v11i3.932 ISSNp: 2488-9229; ISSNe: 3027-1118
IJSGS FUGUSAU VOL. 11(3) WEBSITE: https://fugus-ijsgs.com.ng

this research would not only be essential for controlling fluid flow in microchannels but would also aid in the addition and removal of reactants during chemical reactions. Additionally, by understanding these interplays, the outcome of the work can serve as a guide for the design of advanced heat control mechanisms for applications involving high-performance and microfluidic equipment.

2.0 DESCRIPTION OF THE FLOW

We consider buoyancy-induced flow of an incompressible fluid in an up-facing slit microchannel with parallel plates. The channel is coated with a porous medium and exponential heat generation, causing the fluid to rise. The two plates in the microchannel are intentionally modified such that one plate has SHS and the other has a no-slip surface, both exposed to a transverse magnetic field, as illustrated in Figure 1. The coordinate system is defined with the X-axis aligned with the flow direction and gravitational force (g), while the Y-axis represents the perpendicular direction. A uniform magnetic field of specified strength is introduced perpendicular to the plates.

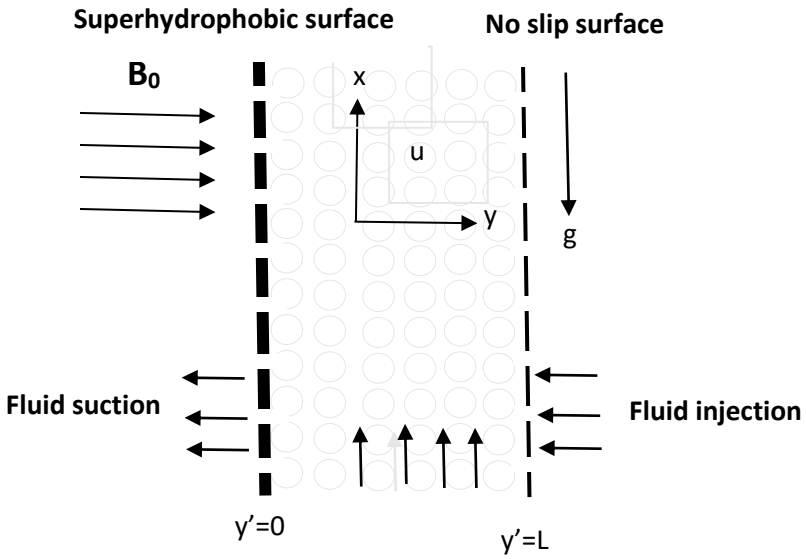

Figure 1: Schematic Diagram of the Flow

The study considers two cases: one where the SHS is heated and the other one where the NSS is heated. Building on the work of Hamza *et al.* (2025), we have incorporated suction/injection and a porous medium into the governing momentum equation and introduced an exponential heat source parameter into the temperature component. The dimensional equations for the current model can be written as

$$v\frac{d^2u}{dy^2} + V_0\frac{du}{dy} + g\beta(T - T_0) - \frac{1}{K}u - \frac{vB_0^2u}{\rho} = 0 \quad (1)$$

$$\frac{k}{\rho C_P}\frac{d^2T}{dy^2} + V_0\frac{dT}{dy} + \frac{q_e(T_h - T_0)}{\rho C_P}exp(-nyL^{-1}) = 0 \quad (2)$$

Subjected to following boundary conditions

$$\left.\begin{aligned} T(y) &= A(T_h - T_0) + \gamma'\frac{dT}{dy} \\ u(y) &= \lambda'\frac{du}{dy} \end{aligned}\right\} \text{ at } y = 0 \quad (3)$$

$$\left.\begin{aligned} T(y) &= T_0 + B(T_h - T_0) \\ u(y) &= 0 \end{aligned}\right\} \text{ at } y = L \quad (4)$$

With dimensionless quantities as

$$\left.\begin{aligned} (Y,\gamma,\lambda) &= \frac{(y,\gamma',\lambda')}{L}, \quad \theta = \frac{T - T_1}{T_2 - T_1}, \quad Q = \frac{q_eL^2}{k}, \quad U = \frac{uv}{g\beta L^2\left[T_2 - T_1\right]}, \\ M^2 &= \frac{\sigma B_0^2L^2}{\rho\upsilon}, \quad Da = \frac{vk}{L^2}, \Pr = \frac{v\rho C_P}{k}, \quad S_J = \frac{V_0L}{v} \end{aligned}\right\} \quad (5)$$

Putting equation (5) into equations (1) and (2), we get

DOI: https://doi.org/10.57233/ijsgs.v11i3.932 ISSNp: 2488-9229; ISSNe: 3027-1118
IJSGS FUGUSAU VOL. 11(3) WEBSITE: https://fugus-ijsgs.com.ng

$$\frac{d^2U}{dY^2} + S_J \frac{dU}{dY} - M_1^2 U + \theta = 0 \quad (6)$$

$$\frac{d^2\theta}{dY^2} + S_J\, Pr \frac{d\theta}{dY} + Q\, exp(-nY) = 0 \quad (7)$$

Substituting non-dimensionless quantities into equations (3) and (4), we get

$$\left.\begin{aligned}\theta(Y) &= A + \gamma \frac{d\theta}{dY} \\ U(Y) &= \lambda \frac{dU}{dY}\end{aligned}\right\} \quad \text{at } Y = 0 \quad (8)$$

$$\left.\begin{aligned}\theta(Y) &= B \\ U(Y) &= 0\end{aligned}\right\} \quad \text{at } Y = 1 \quad (9)$$

Case I: When SHS is heated $(A = 1, B = 0)$
Case II: When NSS is heated $(A = 0, B = 1)$

3.0 METHODOLOGY

Solving equations (6) and (7) in steady-state form using the theory of simultaneous equations, the solutions of energy and momentum have been obtained as

$$\theta(y) = D_1 + D_2\, exp\left(-S_J\, Pr\, Y\right) + D_3\, exp(-nY) \quad (10)$$

$$U(Y) = D_4\, exp(M_3 Y) + D_5\, exp(-M_4 Y) + D_6 + D_7\, exp\left(-S_J\, Pr\, Y\right) + D_8\, exp(-nY) \quad (11)$$

The solution to the Volume flow rate is obtained as:

$$Q_n = \int_0^1 U(Y)dY = \frac{D_4 K_1}{M_3} + \frac{D_5 K_2}{M_4} + D_6 + \frac{D_7 K_3}{S_J Pr} + \frac{D_8 K_4}{n} \quad (12)$$

The skin friction and Nusselt Number for both plates is also determined as:

$$\left.\frac{dU}{dY}\right|_{Y=0} = D_4 M_3 - D_5 M_4 - D_7 S_J\, Pr - D_8 n \quad (13)$$

$$\left.\frac{dU}{dY}\right|_{Y=1} = D_4 M_3\, exp(M_3) - D_5 M_4\, exp(-M_4) - D_7 S_J\, Pr exp(-S_J\, Pr) - D_8 n\, exp(-n) \quad (14)$$

$$\left.\frac{d\theta}{dY}\right|_{Y=0} = -D_2 S_J\, Pr - D_3 n \quad (15)$$

$$\left.\frac{d\theta}{dY}\right|_{Y=1} = -D_2 S_J\, Pr\, \exp\left(-S_J \mathrm{Pr}\right) - D_3 n\, exp(-n) \quad (16)$$

4.0 RESULTS AND DISCUSSION

The steady-state analysis of the wall porosity effect on buoyancy-driven flow with exponential heat generation in a porous SHO microchannel is performed. The effects of the key parameters, namely, exponential heat source parameter (Qs), suction/injection (Sj), velocity slip parameter (λ), and temperature jump parameter, embedded in the flow pattern, have been discussed given their possible applications. The solutions of the governing equations in terms of temperature, velocity, volume flow rate, skin friction, and Nusselt number have been determined using the theory of simultaneous differential equations. Some illustrative graphs have also been plotted using MATLAB software (Version R2021a) to describe various flow characteristics. It is important to state that Sj < 0 represents fluid injection, while Sj > 0 denotes fluid suction.

The impact of suction/injection on temperature and velocity profiles is described in Figures 3(a, b) and 4(a, b), respectively, for both cases. From these figures, it is evident that increasing values of the injection parameter promote the thermal and hydromagnetic flows, whereas fluid suction does the opposite. Suction/injection factors contribute significantly to boundary layer control, such as in engineering, aerodynamics, space research, and medicine. Therefore, the outcome of these findings can be very useful for controlling fluid flow in channels as well as aiding the addition and removal of reactants during chemical reactions. Figures 5(a, b) and 6(a, b) explain the flow pattern when the exponential heat source parameter is varied on the energy and momentum components, respectively. It is worth mentioning that both the fluid temperature and velocity demonstrate an increasing tendency for cases I and II when the level of Qg is raised. This is inherently true since the system may be able to transfer heat more quickly because of the exponential growth of the extra heat boost. Additionally, it is assumed that the heat generation parameter near the plate conveys additional heat, increasing the fluid flow rate and, thus, the temperature and velocity distributions across the boundary layer region. Increasing efficiency, performance, and safety in a wide range of applications is made possible by the ability to regulate velocity flow in both SHS and NSS that are being heated by manipulating exponential heat source parameters. Numerous industries, including energy, transportation, construction, and healthcare, will be significantly impacted by these discoveries.

The impact of the suction/injection parameter with the temperature jump on the volume flow rate is plotted in Figure 7(a, b) for both case I and case II, respectively. It was established in case I that the function of the fluid

DOI: https://doi.org/10.57233/ijsgs.v11i3.932

ISSNp: 2488-9229; ISSNe: 3027-1118

IJSGS FUGUSAU VOL. 11(3) WEBSITE: https://fugus-ijsgs.com.ng

injection parameter is to escalate the fluid flow rate as the temperature jump impact rises, while a counter attribute is noticed in the application of fluid suction. In case II, the fluid injection is observed to bring down the volume flow rate, whereas increasing the fluid suction parameter produced a reverse effect.

The deviations of suction/injection impact on the rate of heat transfer and skin friction affected by velocity slip and temperature jump conditions are demonstrated in Figures 8 to 11. The characteristic behaviour of the rate of heat transfer, also known as the Nusselt number, is plotted in Figures 8(a, b) and 9(a, b) for both case I and case II, respectively. In case I, it is revealed that an increase in the heat transfer rate is evident when the fluid injection parameter is increased, as displayed in Figure 8a at (y=0). In the presence of the fluid suction parameter, a contrast behaviour is noticed as shown in Figure 8b. In case II, the opposite effect of case I happens for the actions of suction and injection.

Figures 10 (a, b) and 11 (a, b) display the significant influence of suction/injection on shear stress. In both cases I and II, when SHS and NSS are heated respectively, it was depicted that the skin friction is strengthened for higher injection parameters, but an opposite effect is seen in the presence of suction parameters at the lower plate as shown in Figures 10a and 11a. In the upper surface at y=1, a reverse phenomenon happens as illustrated in Figures 10b and 11b. There are, however, observed points of intersection in Figures 10a and 11a.

4.1 Results Validation

In order to verify the accuracy and precision of the present work, Figure 2 was plotted to showcase the relationship between our work and that of Hamza *et al.* (2025) for the limiting case when $Sj = 0$ and $Da = 10000$. An excellent agreement was established.

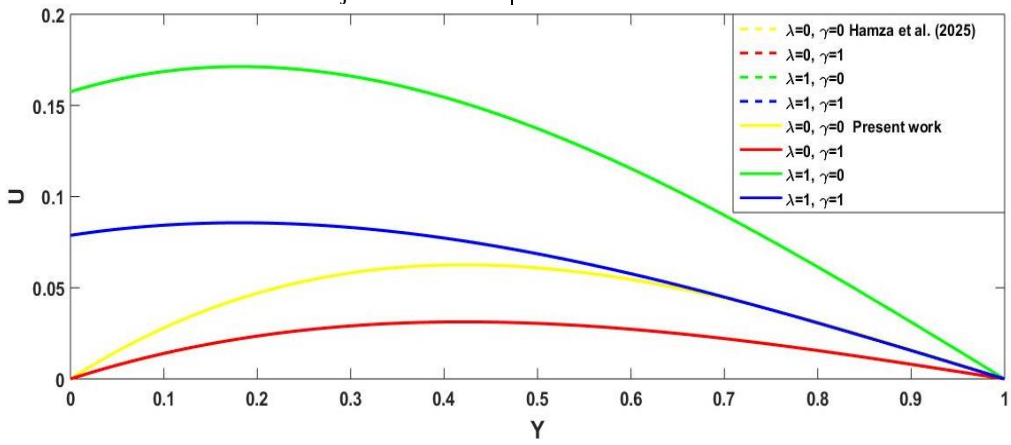

Figure 2: Graphical comparison between the Work of Hamza *et al.* (2025) and the Present Work for the limiting case

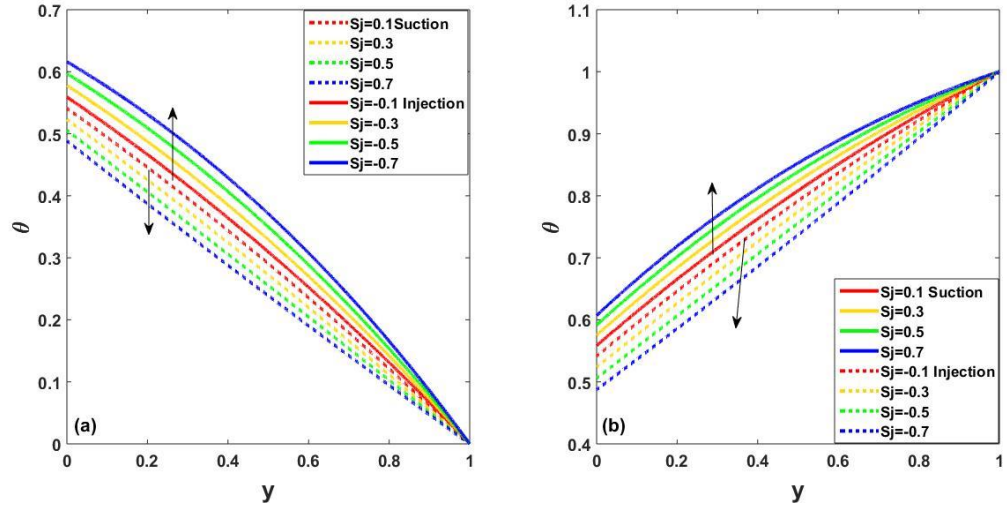

Figure 3: Variation of Sj on Temperature Profile for (a) Case I and (b) Case II

DOI: https://doi.org/10.57233/ijsgs.v11i3.932 ISSNp: 2488-9229; ISSNe: 3027-1118
IJSGS FUGUSAU VOL. 11(3) WEBSITE: https://fugus-ijsgs.com.ng

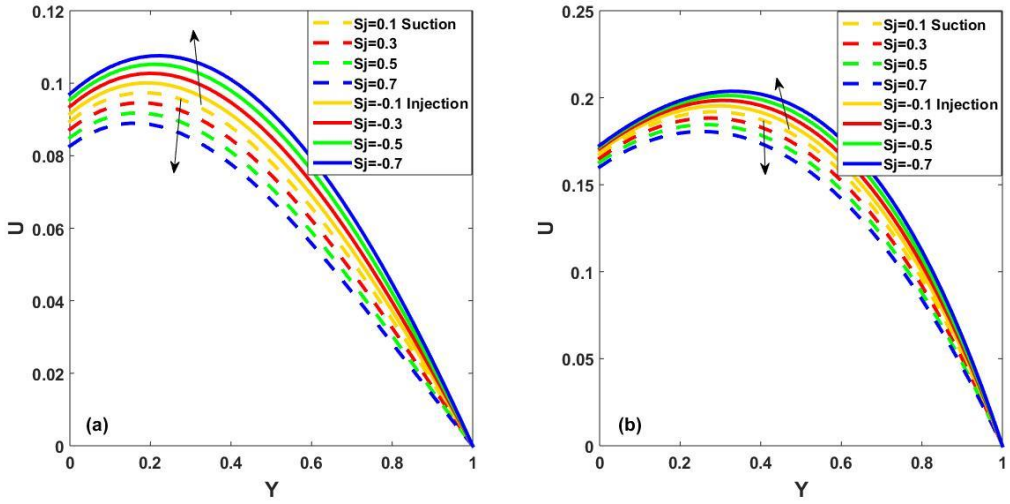

Figure 4: Variation of Sj on Velocity Profile for (a) Case I and (b) Case II

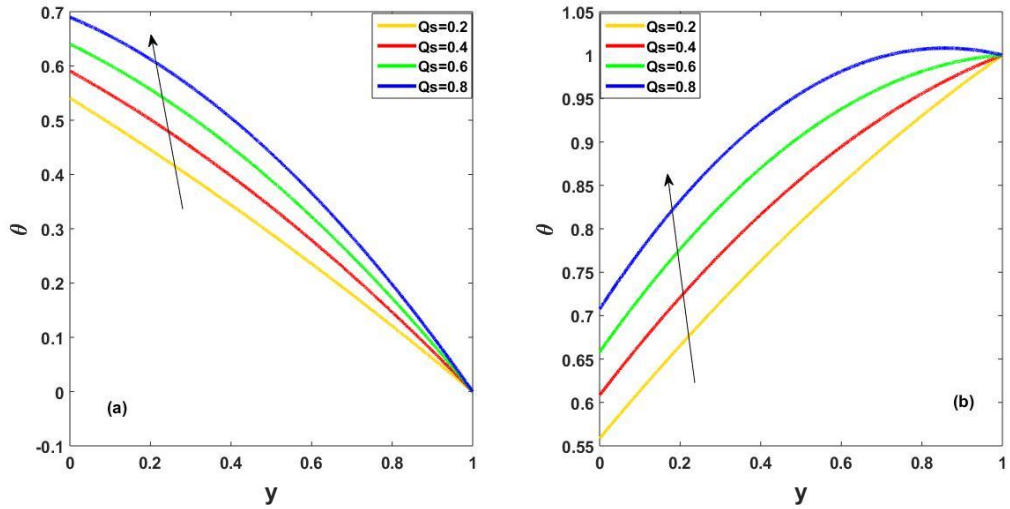

Figure 5: Variation of Qs on Temperature Profile for (a) Case I and (b) Case II

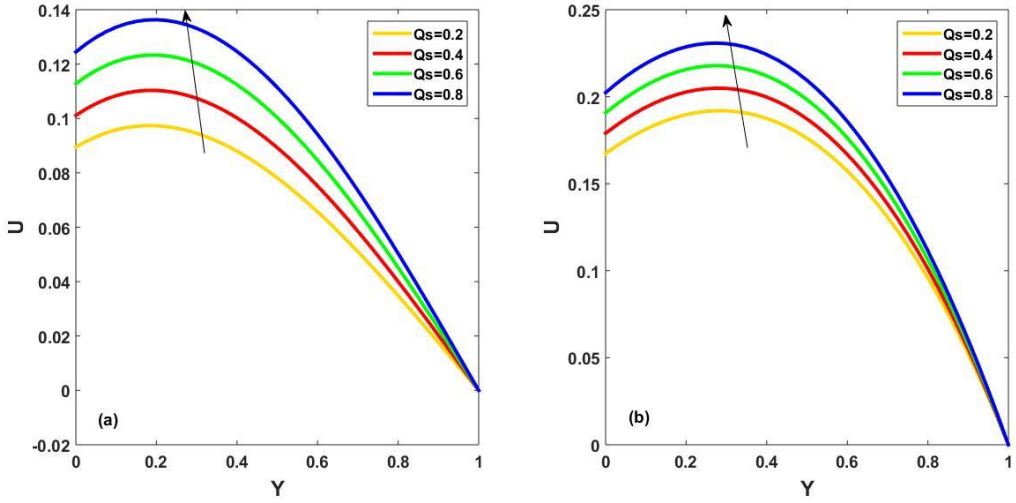

Figure 6: Variation of Qs on Velocity Profile for (a) Case I and (b) Case II

DOI: https://doi.org/10.57233/ijsgs.v11i3.932 ISSNp: 2488-9229; ISSNe: 3027-1118
IJSGS FUGUSAU VOL. 11(3) WEBSITE: https://fugus-ijsgs.com.ng

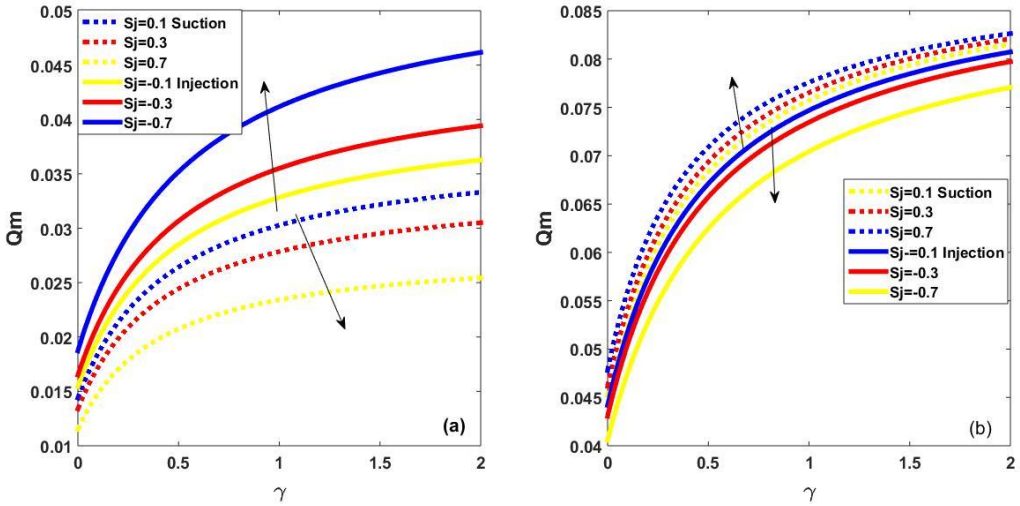

Figure 7: Variation of Sj on Volume Flow Rate for (a) Case I and (b) Case II

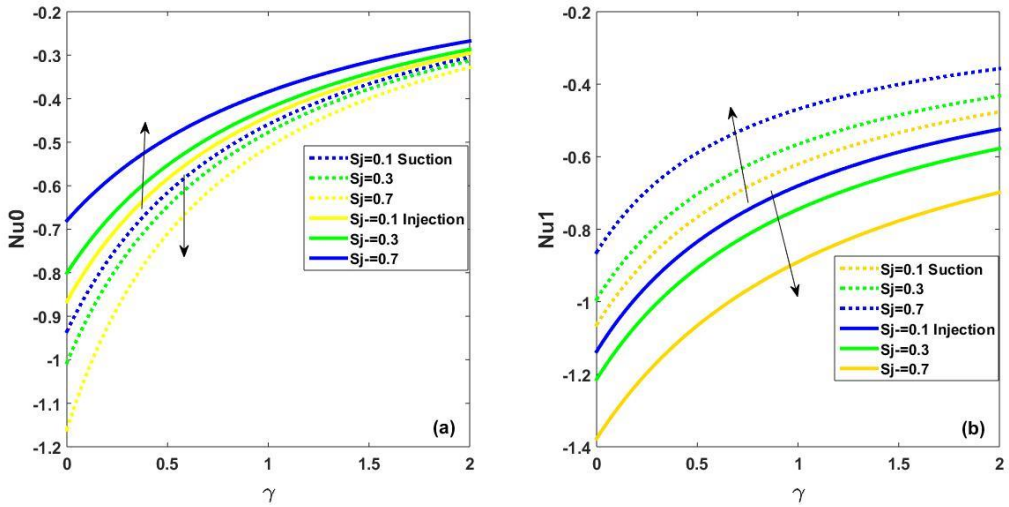

Figure 8: Variation of Sj on Nusselt number for Case I at the (a) lower and (b) upper walls

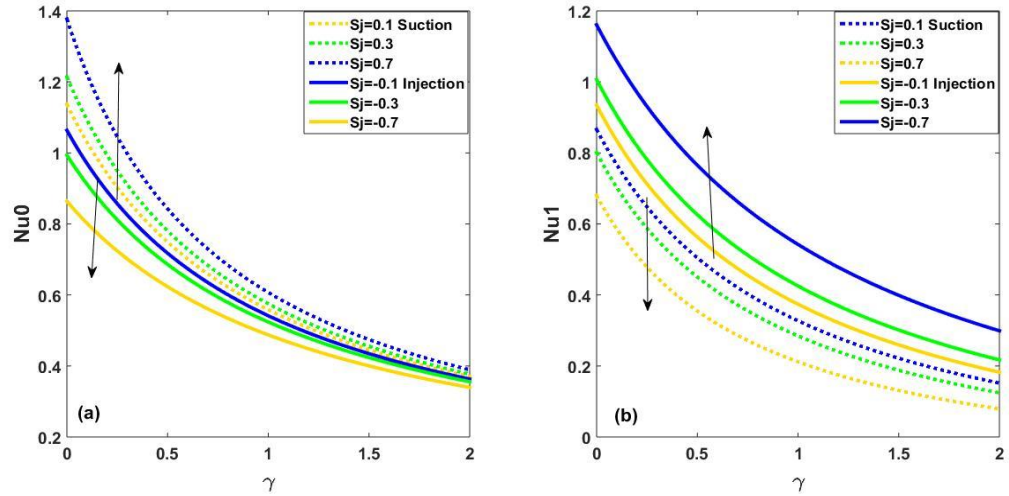

Figure 9: Variation of Sj on Nusselt number for Case II at the (a) lower and (b) upper walls

DOI: https://doi.org/10.57233/ijsgs.v11i3.932 ISSNp: 2488-9229; ISSNe: 3027-1118
IJSGS FUGUSAU VOL. 11(3) WEBSITE: https://fugus-ijsgs.com.ng

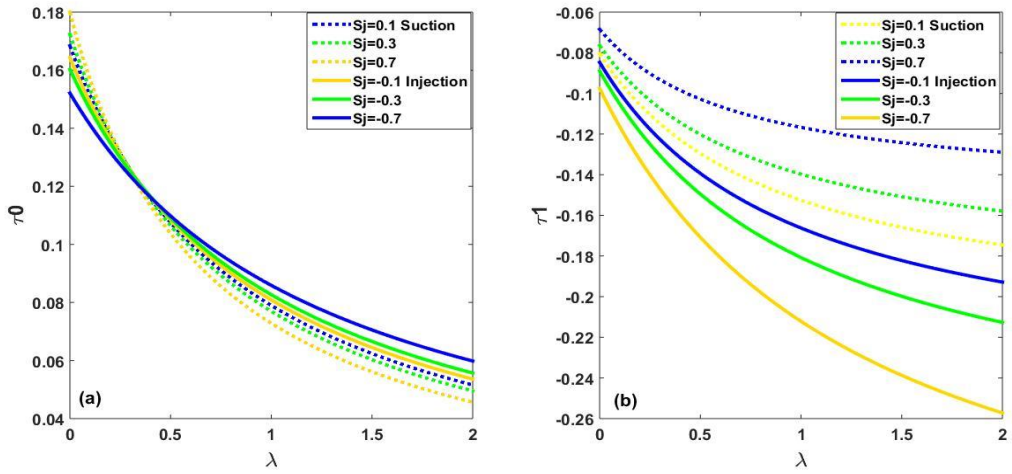

Figure 10: Variation of Sj on Skin Friction for Case I at the (a) lower and (b) upper walls

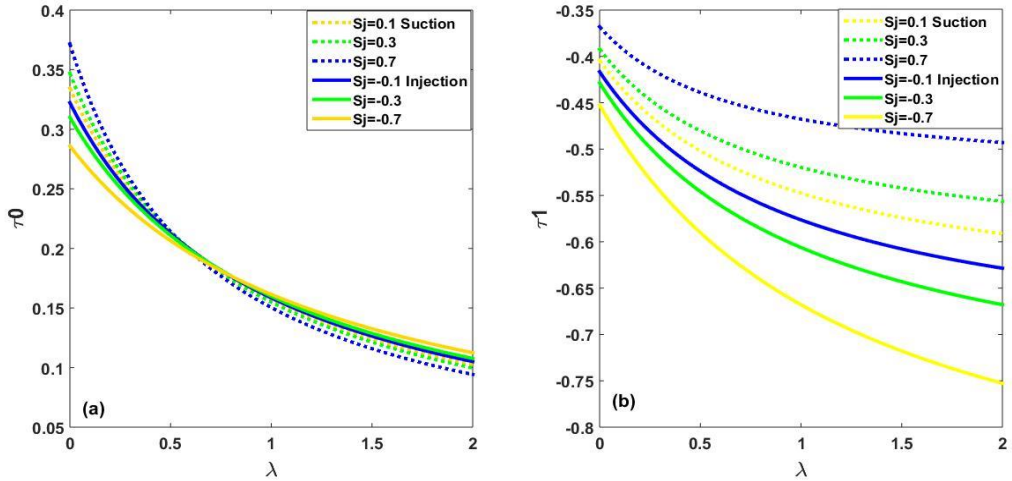

Figure 11: Variation of Sj on Skin Friction for Case II at the (a) lower and (b) upper walls

5.0 CONCLUSION

This work evaluates the significance of wall porosity on buoyancy-induced flow of an incompressible fluid in a porous SHS microchannel instigated by exponential heat generation. The resultant governing equations representing the temperature and velocity components are treated analytically using the theory of simultaneous differential equations. Additionally, the physical component of engineering interest, namely volume flow rate, skin friction, and Nusselt number expressions, has also been determined. Analysis graphs have been plotted to elucidate the influences of key parameters such as Sj, Qs, and on the flow dynamics, facilitating a comprehensive understanding of their individual and synergistic effects. Comprehending the temperature variations on surfaces coated with pores is very instrumental for effective heat management in the electronics, aerospace, and automotive industries. The major results from this study are stated below:

i. Increasing the fluid injection parameter encourages the thermal and hydromagnetic flow in both cases, while a reverse effect occurs in the presence of the fluid suction parameter.

ii. The temperature and velocity distributions increase in both case I and case II with a rise in Qs.

iii. In the presence of, volume flow rate increases/decreases with an increase/decrease in Sj in case I, but produces an opposite effect in case II.

iv. In case I, the rate of heat transfer is increased by raising the fluid injection parameter at the lower surface (y=0) but reducing it at the upper wall (y=1). An opposite effect occurs in case II.

v. In both cases, the skin friction demonstrates an increasing trend in the action of fluid injection at the lower surfaces (y=0), whereas a counter behavior is seen in the presence of fluid suction at (y=1).

vi. In the future, this work will be extended to study the impact of the nonlinear thermal variable.

REFERENCES

Adeyemo, A., Sibanda P., and Goqo S. (2024). Analysis of heat and mass transfer of a non-linear convective heat generating fluid flow in a porous medium with variable viscosity. Scientific African, e02140. doi: 10.1016/j.sciaf.2024.e02140

Ajibade, A. O., Gambo J. J. and Jha B. K. (2023). Effects of viscous and Darcy dissipation on fully developed natural convection flow in a composite channel partially filled with porous material: Homotopy perturbation method (HPM), Journal of Applied Mathematics and Mechanics, 103(6), https//doi.org/10.1002/zamm.202100583

Akhtari, M. R. and Karimi N. (2020). Thermohydraulic analysis of a microchannel with varying superhydrophobic roughness, Applied Thermal Engineering, 172. https://doi.org/10.1016/j.applthermaleng.2020.115147

Allan, M. M. and Dardery S. M. (2018). On the effect of convective heat and mass transfer on unsteady mixed convection MHD flow through vertical porous medium. International Journal of Latest Research in Engineering and Technology, 13, 66-78, 2018. https://doi.org/10.5897/IJPS2017.4678.

Bachok, N., Tajuddin, S. N. N., Anuar N. S. and Rosali H. (2023). Numerical computation of stagnation point flow and heat transfer over a nonlinear stretching/shrinking sheet in hybrid nanofluid with suction/injection effects, Journal of Advance Research in Fluid Mechanics and Thermal Sciences, 107(1).

Bordoloi, R., Ahmed, N. and Kakati L. (2021). Dufour effect on three-dimensional flow past a porous vertical plate in a porous medium with periodic suction and permeability. Journal of Heat and Mass Transfer, 24, 283-308. http://dx.doi.org/10.17654/0973576321005.

Bordoloi, R., Chamuah K., and Ahmed N. (2023). Free Convective MHD Radiative Flow Past a Porous Vertical Plate in a Porous Medium with Chemical Reaction, Biointerface Research in Applied Chemistry, 13 (3), pp. 1-15, 2023.

Chakravarty, A., Ghosh, K., Sen, S. and Mukhopadhyay, A. (2022). Impact of liquid coolant subcooling on boiling heat transfer and dryout in heat-generating porous media, Thermal Science and Engineering Progress, 30, 101251. DOI: 10.1016/j.tsep.2022.101251.

Chaudhary R. C. and Jain A. (2007). Combined heat and mass transfer effects on MHD free convection flow past an oscillating plate embedded in porous medium, Romania Journal of Physics, 52, pp. 505–524.

Fathi, M. and Heyhat, M. and Zabetian, M. and Bigham, S. (2023). Porous-fin microchannel heat sinks for future micro-electronics cooling. International Journal of Heat and Mass Transfer, 3, 202. 123662. 10.1016/j.ijheatmasstransfer.2022.123662.

Gireesha B. J. and Sindhu S. (2020). MHD natural convection flow of Casson fluid in an annular microchannel containing porous medium with heat generation/absorption. Nonlinear Engineering, 9, pp. 23-232.

Hamza, M. M., Shuaibu A. and Ahmad S. K. (2022). Unsteady MHD free convection flow of an exothermic fluid in a convectively heated vertical channel filled with porous medium, Scientific Reports, 12, 11989. https://doi.org/10.1038/s41598-022-16064-y

Hamza, M. M., Shehu, A., Muhammad, I., Shuaibu, A., Ojemeri G. (2024a). Electro-kinetically free convective heat flow in a slit microchannel, International Journal of Applied and Computational Mathematics, 10. https://doi.org/10.1007/s40819-024-01765-x.

Hamza, M. M., Shehu, A., Muhammad, I., Shuaibu, A., Ojemeri G. (2024b). Electrokinetically controlled mixed convective heat flow in a slit microchannel", Heat Transfer, DOI:10.1002/htj.23104.

Hamza M. M., Sani D. and Ojemeri G. (2024c). Numerical evaluation of wall porosity on hydromagnetic slip flow due to variable thermal conductivity", Journal of Engineering and Technology (JET), 15(2), pp. 1-23.

Hamza, M. M., Tsafe, A. M., Ahmad, S. K., Abdullahi M. B. (2025). Impact of Magnetized Exponential Heat Generating Fluid in a Superhydrophobic Microchannel, Int. J. Appl. Comput. Math, 11, 138.

Heidarian, A., Rafee, R., and Valipour, M. S. (2020). Effects of wall hydrophobicity on the thermohydraulic performance of the microchannels with nanofluids, Int. Comm. Heat and Mass Transfer, 117. https://doi.org/10.1016/j.icheatmasstransfer.2020.104758

Jha, B. K. and Gwandu B. J. (2018). MHD free convection flow in a vertical slit micro-channel with superhydrophobic slip and temperature jump: Heating by constant wall temperature, Alexandria Engineering Journal, 57. https://dx.doi.org/10.1016/j.aej.2017.08.022

Jha, B. K. and Gwandu B. J. (2020). MHD free convection flow in a vertical porous super-hydrophobic microchannel, J. Proc. Mech. Eng., 235 (2).

Jha, B. K., Altine M. M. and Hussaini, A. M. (2022). Role of suction/injection on free convective flow in a vertical channel in the presence of point/line heat source/sink, ASME Journal of Heat Transfer, 144, 062602.

Jha, B. K., Azeez L. A. and Oni M. O. (2019). Unsteady Hydromagnetic-Free convection flow with suction/injection, Journal of Taibah University, 13, 136–145.

Jha, B. K., Isah, B. Y. and Uwanta I. J. (2018). Combined Effect of Suction/Injection on MHD Free-Convection Flow in a Vertical Channel with

Thermal Radiation, Ain Shams Engineering Journal, 9(4), 1069–1088.

Kadeethum, T., Ballarin, F., Choi, Y., O'Malley, D., Yoon H. and Bouklas N. (2022). Non-intrusive reduced order modelling of natural convection in porous media using convolutional autoencoders: comparison with linear subspace techniques, Advances in Water Resources, 160, 104098.

Kamis, N. I. Rawi, N. A., Jiann, L. Y., Shafie S. and Ilias M. R. (2023). Thermal characteristics of an unsteady hybrid nano-Casson fluid passing through a stretching thin-film with mass transition, Journal of Advance Research in Fluid Mechanics and Thermal Sciences, 104(2).

Kamis, N. I., Bashir, Md. F., Shafie, S., Khairuddin T. K. A. and Jiann L. Y. (2021). Suction effect on an unsteady Casson hybrid nanofluid film past a stretching sheet with heat transfer analysis, IOP Conferenece Series: Materials Science and Engineering, 1078.

Kamis, N. I., Jiann, L. Y., Shafie, S., Khairuddin T. K. A. and Faisal Md. B. (2022). Magnetohydrodynamics boundary layer flow of hybrid nanofluid in a thin film over an unsteady stretching permeable sheet, Journal of Nanofluid, 11(1), 74-83.

Karouei, S. H. H., Shani, M. B., Sekaloo, M., Eimeni, S. H. H., Pasha, P., and Ganji D. D. Computational modelling of magnetized hybrid nanofluid flow and heat transfer between parallel surfaces with suction/injection, International Journal of Thermofluids, 22, 100613.

Khalid, A., Khan I. and Khan A. (2015). Unsteady MHD free convection flow of Casson fluid past over an oscillating vertical plate embedded in a porous medium, Engineering Sciences and Technology, 18, 309–317.

Lee, H., Fridlind A. M. and Ackerman A. S. (2021). An evaluation of size-resolved cloud microphysics scheme numerics for use with radar observations, Part II: condensation and evaporation, J. Atmos. Sci., 78(5), 1629-1645. DOI:10.1175/JAS-D-20-0213.1.

Mishra, A. K., Paul T. and Singh A. K. (2022). Mixed convention flow in a porous medium bounded by two vertical walls, Forsch Ingenieurwes, 67, 198–205.

Nihall, K., Mahabaleshwar, U. and Joo S. (2024). Darcy Forchhiemer imposed exponential heat source-sink and activation energy with the effects of bioconvection over radially stretching disc, Scientific Report. 2024, https://doi.org/10.1038/s41598-024-58051-5.

Ojemeri G. and Onwubuya I. O. (2023c). Significance of viscous dissipation and porosity effects in a heated superhydrophobic microchannel, Journal of Engineering and Technology (JET), 14(2), pp. 1-19.

Ojemeri, G. and Onwubuya I. O. (2023a). Exploring the dynamics of viscous dissipative fluid past a super-hydrophobic microchannel in the coexistence of mixed convection and porous medium", Saudi Journal of Engineering Technology, 8, pp.71-80.

Ojemeri, G. and Onwubuya I. O.(2023b). Analysis of mixed convection flow on Arrhenius-controlled heat generating/absorbing fluid in a superhydrophobic microchannel: A semi-analytical approach, Dutse Journal of Pure and Applied Sciences, 9a, 344-357.

Ojemeri, G., Onwubuya, I. O., Omokhuale, E., Hussaini A. and Shuaibu A. (2024). Analytical investigation of Arrhenius kinetics with heat source/sink impacts along a heated superhydrophobic microchannel, UMYU Scientifica, 3(1), 61-71. DOI:105619/usci.2431.004

Sharma, H., Gaddam, A., Agrawal, A., Joshi, S.S. and Dimov, S. S. (2020). Influence of texture shape and arrangement on thermo-hydraulic performance of textured microchannels, Int. J. Therm. Sci., 147. https://doi.org/10.1016/j.ijthermalsci.2019.106146.

Sia, G. D., Lim, C.S., Tan, M. K., Chen, G. M. and Hung, Y. M. (2023). Anomalously enhanced subcooled flow boiling in superhydrophobic graphene-nanoplatelets'-coated microchannels, Int. Comm. Heat and Mass Transfer, 146. https://doi.org/10.1016/j.icheatmasstransfer.2023.106932

Uwanta I. J. and Hamza M. M. (2014). Effect of Suction/Injection on Unsteady hydro-magnetic Convective Flow of Reactive Viscous Fluid Between Vertical Porous Plates with Thermal Diffusion, International Scholarly Research, Article ID 980270, 1–14.

Yale, I. D., Uchiri, A. M. T., Hamza M. M., and Ojemeri G. (2023). Effect of viscous dissipation fluid in a slit microchannel with heated superhydrophobic surface, Dutse Journal of Pure and Applied Sciences, 9(3b), pp. 290-302.

Zhang, W, Wang, Q., Zeng, M., and Zhao, C. (2019). Thermoelectric effect and temperature- gradient-driven electrokinetic flow of electrolyte solutions in charged nanocapillaries, International Journal of Heat and Mass Transfer, 143. https://doi:10.1016/j.ijheatmasstransfer.2019.118569.

Nomenclature

u dimensional vertical velocity of the flow (m/s)

y dimensional horizontal position between the plates (m)

DOI: https://doi.org/10.57233/ijsgs.v11i3.932 ISSNp: 2488-9229; ISSNe: 3027-1118

IJSGS FUGUSAU VOL. 11(3) WEBSITE: https://fugus-ijsgs.com.ng

g gravitational force (m/s^2)
T_1 dimensional temperature of the surrounding (K)
T_2 dimensional temperature higher than T_0 (K)
B_0 constant magnetic field applied (T)
Y dimensionless horizontal position between the plates (-)
U dimensionless vertical velocity of the flow (-)
M magnetic parameter (-)
Da Darcy number
S Suction/injection parameter
L channel width (m)
Qv dimensionless volume flow rate (-)
Nu Nusselt number (-)
Qs exponential heat source parameter
n exponential index
k thermal conductivity (W/nK)

Greek symbols

γ' dimensional temperature jump (m)
γ dimensionless temperature jump (-)
λ' dimensional slip length (m)
λ dimensionless slip length (-)
τ skin friction coefficient
θ dimensionless temperature (-)
ν fluid kinematic viscosity (m^2/s)
ρ fluid density (kg/m^3)
σ fluid electrical conductivity (A^2S^3/kgm^3)

Appendix

$$M_1=\sqrt{\left(\frac{1}{Da}+M^2\right)}, D_1=A-D_2\left(\gamma S_J\,\mathrm{Pr}+1\right)-D_3\left(\gamma n+1\right), D_2=\frac{A-B-D_3\left(\gamma n+1-\exp(-n)\right)}{\gamma S_J\,\mathrm{Pr}+1-\exp\left(-S_J\,\mathrm{Pr}\right)},$$

$$D_3=\frac{-Q}{n^2-S_J\,\mathrm{Pr}}, M_3=\frac{-S_J+\sqrt{S_J^2+4M_1^2}}{2}, M_4=\frac{S_J+\sqrt{S_J^2+4M_1^2}}{2}, D_6=\frac{D_1}{M_1^2}, D_7=\frac{-D_2}{S_J^2\,\mathrm{P}_r^2-S_J^2\,\mathrm{Pr}-M_1^2},$$

$$D_8=\frac{-D_3}{n^2-S_Jn-M_1^2}, P_1=\lambda M_3-1, P_2=\lambda S_J\,\mathrm{Pr}+1, P_3=\lambda n+1, P_4=1+\lambda M_4,$$

$$D_5=\frac{D_4P_1-D_7P_2-D_8P_3-D_6}{P_4}, P_5=D_6+D_7\exp(-S_J\,\mathrm{Pr})+D_8\exp(-n)$$

$$P_6=P_4\exp(M_3)+P_1\exp(-M_4), P_7=\left(D_7P_2+D_8P_3+D_6\right)\exp(-M_4), D_4=\frac{P_7-P_5P_4}{P_6},$$

$$K_1=\exp(M_3)-1, K_2=1-\exp(-M_4), K_3=1-\exp(-S_J\,\mathrm{Pr}), K_4=1-\exp(-n)$$